

# Journal of Materials Chemistry C

Accepted Manuscript



This is an *Accepted Manuscript*, which has been through the Royal Society of Chemistry peer review process and has been accepted for publication.

*Accepted Manuscripts* are published online shortly after acceptance, before technical editing, formatting and proof reading. Using this free service, authors can make their results available to the community, in citable form, before we publish the edited article. We will replace this *Accepted Manuscript* with the edited and formatted *Advance Article* as soon as it is available.

You can find more information about *Accepted Manuscripts* in the [Information for Authors](#).

Please note that technical editing may introduce minor changes to the text and/or graphics, which may alter content. The journal's standard [Terms & Conditions](#) and the [Ethical guidelines](#) still apply. In no event shall the Royal Society of Chemistry be held responsible for any errors or omissions in this *Accepted Manuscript* or any consequences arising from the use of any information it contains.

# Development of Strongly Absorbing *S,N*-Heterohexacene-Based Donor Materials for Efficient Vacuum-Processed Organic Solar Cells

Christoph Wetzel,<sup>a</sup> Amaresh Mishra,<sup>a</sup> Elena Mena-Osteritz,<sup>a</sup> Karsten Walzer,<sup>b</sup> Martin Pfeiffer,<sup>b</sup> Peter Bäuerle<sup>a\*</sup>

<sup>a</sup>Institute of Organic Chemistry II and Advanced Materials  
University of Ulm, Albert-Einstein-Allee 11, 89081 Ulm, Germany

\*E-mail: peter.baeuerle@uni-ulm.de

<sup>b</sup>Heliatek GmbH, Treidlerstrasse 3, 01139 Dresden, Germany

Keywords: heteroacenes, organic semiconductors, planar-heterojunction solar cells, bulk-heterojunction solar cells, vacuum-processing

## Abstract

A series of terminal dicyanovinylene (DCV)-substituted *S,N*-heterohexacenes with variable length of alkyl chains were synthesized and characterized for application in vacuum-processed planar-heterojunction and bulk-heterojunction organic solar cells. X-ray single crystal analysis of hexyl-substituted derivative **4** revealed that the molecules are ordered in columns via  $\pi$ - $\pi$ -stacking. While the influence of the alkyl chain length is negligible on the optoelectronic properties, an odd-even effect was observed with respect to the photovoltaic performance. Vacuum-processed planar-heterojunction organic solar cells prepared using DCV-substituted *S,N*-heterohexacenes as electron donors and C<sub>60</sub> as acceptor showed extraordinary high efficiencies of up to 5.0%. Bulk-heterojunction solar cells incorporating pentyl derivative **3** and C<sub>60</sub> led to excellent power conversion efficiencies of up to 7.1% exceeding those of previously reported *S,N*-heteropentacenes.

## Introduction

In the last decade, great progress has been made in the field of organic solar cells induced by both, the development of new organic semiconductors and the optimization of device fabrication, leading to power conversion efficiencies (PCE) exceeding 10% for solution-processed bulk-heterojunction solar cells utilizing either polymeric or oligomeric donor materials.<sup>1-14</sup> Despite the high efficiencies obtained in both classes, oligomers, often referred to as “small molecules”, exhibit various benefits towards their polymer counterparts such as high reproducibility on both, syntheses and devices, due to their defined and monodisperse structure.<sup>15-17</sup> An additional advantage of oligomers is that they can be processed by thermal evaporation techniques,<sup>18</sup> which avoids the application of toxic and environmentally hazardous chlorinated solvents frequently used for the preparation of solution-processed solar cells. Effective vacuum-processed single junction cells with high PCEs were achieved by, e.g., implementing sexithiophene in combination with subphthalocyanines in planar-heterojunction (PHJ) structures,<sup>19</sup> and unsymmetrical donor (D)-acceptor (A) oligomers comprising strong dipole moments,<sup>20-23</sup> or symmetrical A-D-A oligomers in bulk-heterojunction (BHJ) structures.<sup>18,24-33</sup> Furthermore, processing by thermal evaporation allows the deposition of highly pure and well-defined layers which is beneficial for the construction of multilayered solar cells, e.g., tandem or triple cells.<sup>34</sup> In this respect, vacuum-processed triple cells with a certified PCE of 12.0% were recently reported by us<sup>35</sup> and of 11.1% by Forrest and co-workers.<sup>36</sup>

In our search and development of novel strong absorbers and organic semiconductors, we recently introduced a series of *S,N*-heteroacenes consisting of fused thiophene-pyrrole rings as a novel class of materials. These heteroacenes can be regarded as nitrogen-bridged oligothiophenes and are therefore highly planarized and rigidified. By combining the high stability of oligothiophenes and the favorable physical properties of acenes, they showed largely increased extinction coefficients compared to the non-bridged counterparts.<sup>37</sup> Acceptor-functionalized *S,N*-heteropentacenes (SN5) were implemented in different types of organic and hybrid organic solar cells and achieved efficiencies of 6.5% in vacuum-<sup>38</sup> and 4.9% in solution-processed solar cells.<sup>39</sup> Furthermore, fine-tuned derivatives of this SN5-type showed promise as hole transporter and absorber in perovskite solar cells reaching a PCE of 16.9%.<sup>40-42</sup>

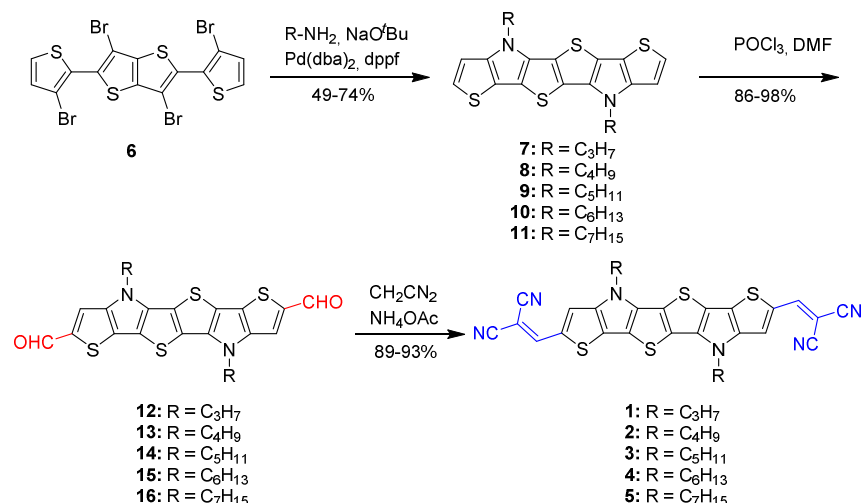
In the continuation of this approach to *S,N*-heteroacenes, we elongated the conjugated  $\pi$ -system to a *S,N*-heterohexacene<sup>43</sup> by replacing the middle thiophene core of *S,N*-heteropentacenes by a thieno[3,2-*b*]thiophene unit. Recently, Wong and co-workers reported efficiencies of up to 3.0% in vacuum-processed organic solar cells incorporating a DCV end-capped *S,N*-heterohexacene comprising branched alkyl side chains as donor material.<sup>44</sup> Furthermore, for

the DCV-substituted *S,N*-heterohexacene good charge carrier mobilities of up to  $0.02 \text{ cm}^2 \text{ V}^{-1} \text{ s}^{-1}$  have been measured in organic field effect transistors (OFET)<sup>43</sup> underlining the concept that incorporation of thieno[3,2-*b*]thiophene units in oligomers<sup>45,46</sup> or polymers<sup>47,48</sup> leads to high charge carrier mobilities. The group of McCulloch reported efficient donor-acceptor polymers for organic solar cells using a hexafused building block, which comprised a thieno[3,2-*b*]thiophene core, resulting in PCEs of up to 5.5% in solution-processed BHJ solar cells.<sup>49</sup>

In this contribution, we now report synthesis, characterization, and photovoltaic properties of a series of DCV end-capped *S,N*-heterohexacenes, in which the length of the alkyl chains attached to the nitrogen bridges is varied. Thermal properties, such as melting point and decomposition temperature, and photovoltaic properties are distinctly influenced by the length of the alkyl side chains, while the optical and electrochemical properties remain almost unaffected due to the identical conjugated backbone. The 5.0% efficiency for PHJ solar cells is one of the highest values ever reported for vacuum-deposited planar-heterojunction solar cells. Device optimization of vacuum-processed BHJ solar cells based on *S,N*-heterohexacenes with pentyl side chains as donor and fullerene  $\text{C}_{60}$  as acceptor resulted in excellent power conversion efficiencies of up to 7.1%.

## Synthesis

Synthesis of novel A-D-A-type fused *S,N*-heterohexacenes **1–5** is outlined in Scheme 1. Parent SN6-systems **7–11** were obtained in good yields (49–74%) by Buchwald–Hartwig amination of literature-known tetrabromo derivative **6** with different alkyl amines in the presence of  $\text{Pd}(\text{dba})_2$  as catalyst, dppf as ligand, and sodium *tert*-butoxide as base. Subsequent Vilsmeier–Haack formylation of heterohexacenes **7–11** gave corresponding dialdehydes **12–16** in excellent yields of 86–98%. Finally, Knoevenagel condensation of dialdehydes **12–16** with malonitrile and ammonium acetate provided DCV end-capped target *S,N*-heterohexacenes **1–5** in 89–93% yield.



**Scheme 1:** Synthesis of acceptor-substituted *S,N*-heterohexacenes **1-5**.

## Thermal properties

For the construction of organic solar cells prepared by vacuum-deposition all compounds should possess high thermal stability. Therefore, the melting ( $T_m$ ) and decomposition temperatures ( $T_d$ ) of **1-5** were investigated by differential scanning calorimetry (DSC) (Figure 2a) and thermogravimetric analysis (TGA) (Figure 2b) under an inert atmosphere at a heating rate of 10 °C min<sup>-1</sup>. The  $T_m$  values increased with decreasing length of alkyl side chains indicating strong intermolecular interactions of the molecules in the solid state. TGA measurements confirmed the high thermal stability of *S,N*-heterohexacenes reflected by a  $T_d$  of 447.9 °C for **1**, 428.6 °C for **2**, 411.2 °C for **3**, 382.6 °C for **4**, and 371.1 °C for **5** determined from the onset value of the degradation process.

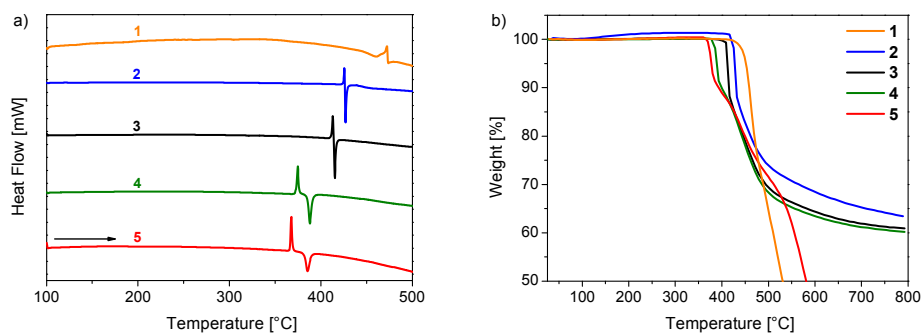


**Figure 2.** a) DSC traces of A-D-A hexacenes **1-5** measured under Ar flow at a heating rate of 10 °C/min; b) TGA traces of A-D-A heterohexacenes **1-5** measured under N<sub>2</sub> flow at a heating rate of 10 °C/min.

## Optical and electrochemical properties

Figure 3 depicts the optical properties of pentyl derivative **3** as an example studied by UV-vis absorption and fluorescence spectroscopy in dichloromethane solution. The data of all derivatives are listed in Table 1. In solution, all compounds **1-5** displayed a strong absorption band between 400 and 620 nm with a maximum at 588 nm and a shoulder at around 547 nm corresponding to an intramolecular charge-transfer transition. The high extinction coefficient of  $160,000 \text{ M}^{-1} \text{ cm}^{-1}$  for heptyl- and hexyl-substituted SN6 derivatives **4** and **5** qualified them as interesting absorbers in vacuum-processed solar cells. The extinction coefficient of oligomers **1-3** could not be determined due to their low solubility. Compared to the shorter homologues DCV-SN3<sup>50</sup> and DCV-SN5,<sup>38,39</sup> the red-shift and intensification of the absorption of DCV-SN6 **1-5** are explained by the elongation of the ring-fused backbone. All derivatives **1-5** showed emission maxima at 628 nm and a shoulder at 678 nm. Because of the planarized molecular backbone Stokes shifts of around  $840$  to  $980 \text{ cm}^{-1}$  were observed for **1-5** indicating a similar geometry in the ground and the first excited state. Lacking differences in the absorption and emission spectra of *S,N*-heterohexacenes **1-5** suggest that the length of the alkyl side chains has negligible influence on the optical properties in solution.

In thin films, all *S,N*-heterohexacenes **1-5** displayed two prominent absorption maxima at 596 nm and 643 nm, which are 50 nm red-shifted compared to the spectra in solution (Figure 3b). This bathochromic shift in thin film absorption can be explained by coplanarization and ordering of the molecules in the bulk suggesting good packing in thin films. The thin film absorption spectra of heterohexacenes **1-5** become slightly broadened and red-shifted ( $\Delta\lambda \leq 9 \text{ nm}$ ) with decreasing length of the alkyl side chains.

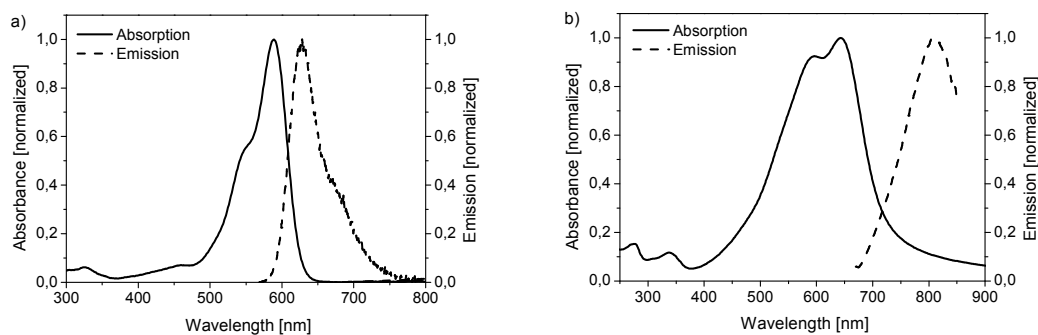


**Figure 3.** (a) UV-vis (solid line) and fluorescence spectrum (dashed line) of DCV-SN6-Pen **3** measured in dichloromethane at 25 °C; (b) Thin film UV-vis (solid line) and fluorescence spectrum (dashed line) of DCV-SN6-Pen **3** prepared by thermal vapor deposition on quartz substrates.

Electrochemical measurements were performed in order to determine HOMO (highest occupied molecular orbital) and LUMO (lowest unoccupied molecular orbital) energy levels. Figure 4 depicts a cyclic voltammogram of oligomer **5** as an example which was measured in 1,2-dichloroethane at 65 °C and the data of derivatives **3-5** are summarized in Table 1. Heterohexacene **5** exhibited two reversible one-electron oxidation waves at 0.56 V and 1.08 V vs. Fc/Fc<sup>+</sup> corresponding to the formation of stable radical cations and dication. In the reductive regime, one irreversible two-electron reduction wave at around -1.38 V vs. Fc/Fc<sup>+</sup> was found. The first oxidation potential of alkylated *S,N*-heterohexacenes **5** is slightly shifted to lower potentials by 0.05 V compared to alkylated *S,N*-heteropentacenes.<sup>38</sup> The reason for this lowering in oxidation potential is the extension of the conjugated  $\pi$ -system by an additional fused thiophene ring. The cyclic voltammograms of oligomers **1** and **2** could not be measured due to their limited solubility.

The HOMO and LUMO energy levels of oligomers **3-5** were calculated from the onset values of the first oxidation and reduction waves applying the standard approximation that the Fc/Fc<sup>+</sup> energy level corresponds to -5.1 eV versus vacuum. The HOMO and LUMO energy levels of *S,N*-heterohexacenes **3-5** were around -5.6 eV and -3.8 eV, respectively, and are basically unaffected by the length of the alkyl side chains which is in agreement with the optical properties. Due to the low-lying HOMO energies of the DCV-SN6 derivatives high open-circuit voltages ( $V_{OC}$ ) are expected in organic solar cells when using C<sub>60</sub> as acceptor.  $V_{OC}$  is typically estimated from the difference of the LUMO energy level of the acceptor and HOMO energy level of the donor minus certain offsets.<sup>51,52</sup>

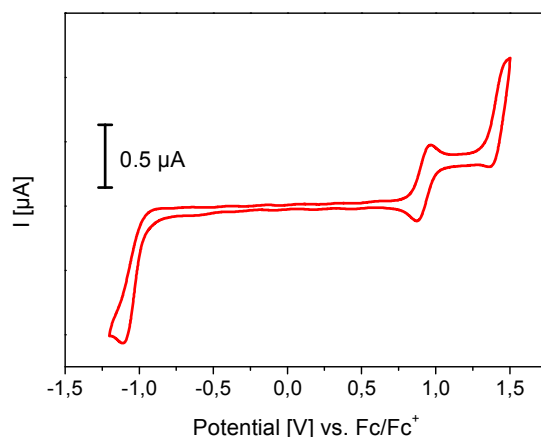


**Figure 4.** Cyclic voltammogram of DCV-SN6-derivative **5** measured in dichloroethane at 65 °C, supporting electrolyte TBAPF<sub>6</sub> (0.1 M), scan rate 100 mV s<sup>-1</sup>, potentials versus Fc/Fc<sup>+</sup> at r.t.



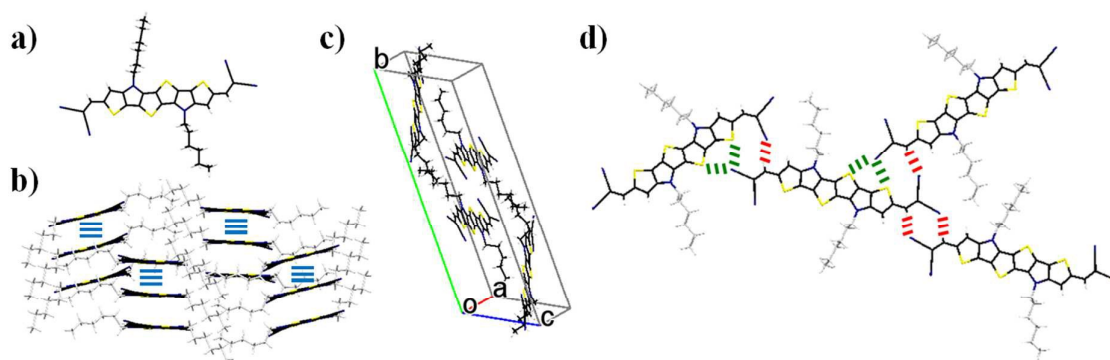
**Table 1.** Optical and electrochemical data of DCV-*S,N*-heterohexacenes **1-5**.

Molecules	$\lambda_{\text{abs sol}}$ [nm] <sup>a</sup>	$\epsilon$ [M <sup>-1</sup> cm <sup>-1</sup> ]	$E_{\text{g}}^{\text{opt sol}}$ [eV] <sup>a</sup>	$\lambda_{\text{em sol}}$ [nm] <sup>a</sup>	Stokes shift [cm <sup>-1</sup> ]	$\lambda_{\text{abs film}}$ [nm] <sup>d</sup>	$E_{\text{g}}^{\text{opt film}}$ [eV]	$E_{\text{ox1}}^0$ [V]	$E_{\text{ox2}}^0$ [V]	$E_{\text{red1}}^0$ [V]	HOMO [eV] <sup>e</sup>	LUMO [eV] <sup>e</sup>	$E_{\text{g}}^{\text{CV}}$ [eV]
<b>1</b>	588 <sup>b</sup>	- <sup>f</sup>	1.97 <sup>b</sup>	631 <sup>c</sup>	979	647, 600	1.72	- <sup>f</sup>	- <sup>f</sup>	- <sup>f</sup>	-	-	-
<b>2</b>	588	- <sup>f</sup>	1.98	627	930	647, 598	1.70	- <sup>f</sup>	- <sup>f</sup>	- <sup>f</sup>	-	-	-
<b>3</b>	589	- <sup>f</sup>	1.98	628	882	643, 596	1.70	0.57	1.08	-1.37	-5.58	-3.83	1.75
<b>4</b>	588	159600	1.98	625	842	638, 591	1.68	0.56	1.06	-1.40	-5.56	-3.78	1.78
<b>5</b>	589	160000	1.98	625	886	640, 594	1.68	0.56	1.08	-1.38	-5.58	-3.77	1.81

<sup>a</sup>Measured in dichloromethane. <sup>b</sup>Measured in 1,1,2,2-tetrachloroethane at 90 °C. <sup>c</sup>Measured in 1,1,2,2-tetrachloroethane at room temperature. <sup>d</sup>Film prepared by thermal vapor deposition. <sup>e</sup>The HOMO and LUMO energy levels were calculated from the onset values of the corresponding redox waves; Fc/Fc<sup>+</sup> was set to -5.1 eV vs. vacuum. <sup>f</sup>Could not be measured due to the limited solubility.

## X-Ray structure analysis











Fractionated sublimation of DCV-SN6 **4** gave blue crystalline needles, which were suitable for single crystal X-ray structure analysis. DCV-SN6 **4** crystallized in the monoclinic space group P 2<sub>1</sub>/c with four equivalent molecules in the unit cell ( $a=4.94184(3)$ ,  $b=32.8876(2)$ ,  $c=19.72071(13)$  Å;  $\alpha=90^\circ$ ,  $\beta=96.1585(6)^\circ$ ,  $\gamma=90^\circ$ ) (Figure 5c). Reduced bond length alternation with an averaged difference of 0.025 Å was observed for the conjugated backbone of DCV-SN6 **4**. The hexyl chains of each molecule, one of which showed weak polymorphism, are directed out of plane in the opposite direction of the planar conjugated backbone (Figure 5a,b). Along the *a*-axis, the molecules order in columns via  $\pi$ - $\pi$ -stacking at distances as short as 3.319 Å (Table 2 and Figure 5b, blue lines). Furthermore, the molecules of DCV-SN6 **4** interact in plane with three neighbour molecules via N-H interactions between the cyano nitrogen and vinylic proton as well as via multiple N-S interactions (Figure 5d and Table 2, red and green lines, respectively).



**Figure 5.** Single-crystal X-ray structure analysis of DCV-SN6-Hex **4**, (a) individual molecule and (b) packing arrangement along *a*-axis. (c) The four molecules packing in the unit cell and (d) intermolecular short contacts of one molecule with its adjacent molecules (view perpendicular to the (2 2 7) plane).



**Table 2.** Short intermolecular distances of DCV-SN6 **4** in the crystal structure.

Atom M1 <sup>a)</sup>	Atom M2 <sup>b)</sup>	Symmetry M1 <sup>a)</sup>	Symmetry M2 <sup>b)</sup>	Distance (Å) <sup>c)</sup>	Length-vdW <sup>d)</sup> (Å)
C29	C8	x,y,z	1+x,y,z	3.396 	-0.004
C35	C24	x,y,z	1+x,y,z	3.319 	-0.081
N30	H10	x,y,z	4-x,1-y,-z	2.447 	-0.303
H10	N30	x,y,z	4-x,1-y,-z	2.447 	-0.303
N16	S4	x,y,z	-2+x,1.5-y,1/2+z	3.028 	-0.322
N16	S7	x,y,z	-2+x,1.5-y,1/2+z	3.125 	-0.225
H8	N78	x,y,z	-2+x,1.5-y,1/2+z	2.480 	-0.27
S4	N16	x,y,z	2+x,1.5-y,-1/2+z	3.028 	-0.322
S7	N16	x,y,z	2+x,1.5-y,-1/2+z	3.125 	-0.225
N78	H8	x,y,z	2+x,1.5-y,-1/2+z	2.480 	-0.27

<sup>a)</sup> Molecule 1. <sup>b)</sup> Molecule 2. <sup>c)</sup> Colour-labelled intermolecular interactions according to Figure 5. <sup>d)</sup> Length of the short distances minus the corresponding van-der-Waals radii.

## Photovoltaic properties

Firstly, we fabricated vacuum-processed PHJ solar cells comprising selective absorber materials **1**, **3**, and **5** using the following layer sequence: ITO/ C<sub>60</sub> (15nm)/ donor (6nm, RT)/ BPAPF (10nm) /BPAPF:NDP9 (45nm, 9.9wt%)/ NDP9 (1nm)/ Au (50nm). The cells utilize organic molecular p-doping (NDP9), which results in loss-free charge extraction to the metal electrode (see experimental section for details).<sup>53</sup>

All devices exhibited high open-circuit voltages ( $V_{OC}$ ) around 0.95 V due to the low-lying HOMO energy levels of the DCV-SN6 derivatives **1**, **3**, and **5** (Table 3). Propyl derivative **1** showed the highest efficiency of 5.0% with a short-circuit current density ( $J_{SC}$ ) of 7.8 mAcm<sup>-2</sup> and a high fill factor (FF) of 67.9%. Further increase in alkyl chain length from propyl to pentyl to heptyl led to a concomitant reduction in the  $J_{SC}$  value which resulted in the lowering of the PCE from 5.0% for propyl **1** to 4.7% for pentyl **3** and 4.3% for heptyl derivative **5**. The 5.0% efficiency shown here represents one of the highest values ever reported for vacuum-deposited planar-heterojunction solar cells.<sup>25,27,30</sup> On the other hand, the FF slightly increased with increasing length of the alkyl side chains. The better  $J_{SC}$  value for **1** can be ascribed to a smaller sterical hindrance offered by the shorter alkyl chains. The reasonably high  $J_{SC}$  and FF values indicate efficient separation of generated excitons at the D:A interface and transport to the respective electrodes. This was further supported by the higher saturation of photocurrent (defined as  $J(-1V)/J_{SC}$ ) indicating a decrease of field-dependent recombination of photogenerated charge carriers.

**Table 3.** Planar-heterojunction solar cells of DCV-substituted heterohexacenes **1**, **3**, and **5**. The active layer thickness is 6 nm.

Donor	$J_{SC}$ [mA cm <sup>-2</sup> ]	$V_{OC}$ [V]	FF	PCE [%]	$R_s$ [ $\Omega$ cm <sup>2</sup> ]	Sat. <sup>a</sup>
<b>1</b>	7.8	0.94	67.9	<b>5.0</b>	4.27	1.08
<b>3</b>	7.2	0.95	68.7	<b>4.7</b>	4.15	1.13
<b>5</b>	6.4	0.95	70.9	<b>4.3</b>	4.08	1.07

<sup>a</sup> Defined as  $J(-1V)/J_{SC}$

BHJ solar cells with DCV-SN6 **1-5** as donor and C<sub>60</sub> as acceptor in a m-i-p-type (metal-intrinsic-p-doped) architecture were prepared by co-evaporation of both compounds at a substrate temperature of 90 °C. For all devices, the following layer sequence was employed: ITO/C<sub>60</sub> (15 nm)/ DCV-SN6 **1-5**:C<sub>60</sub> (20/30 nm, 2:1)/ BPAPF (10 nm)/ BPAPF:NDP9 (45 nm, 10 wt%)/ NDP9 (1 nm)/ Au (50 nm).

The solar cell parameters of DCV-SN6 **1-5** prepared at a substrate temperature of 90 °C with an absorber layer thickness of 20 and 30 nm, respectively, are presented in Table 4. Their current density-voltage ( $J$ - $V$ ) curves are shown in Figure 6a. Characteristic of all  $S,N$ -heterohexacenes **1-5**, the devices containing 20 or 30 nm active layer showed high  $V_{OC}$ s of 0.94 V to 0.97 V for **2-5**, except 0.90 V for **1**. The lower  $V_{OC}$  for **1** was rationalized by partial crystallization of the material in the active layer. The possible closer molecular packing (*vide supra*) may enhance molecular crystallization, which in turn leads to local shunts in the absorber layers. In the crystallites, strong interaction between the molecules also leads to coupling and splitting of the molecular orbitals and consequently to a slight increase of the HOMO energy. For all derivatives, a reduction of FF was observed with increasing active layer thickness from 20 to 30 nm. This shows that the charge carrier collection efficiency decreases with increasing layer thickness in the voltage regime around the maximum power point (MPP). On the other hand,  $J_{SC}$  of **2-5** increased with increasing layer thickness indicating the contribution of the blend layer to the photocurrent generation. Overall, pentyl derivative **3** exceeded the other representatives of the presented  $S,N$ -heterohexacene series resulting in a maximum PCE of 7.1% with a  $J_{SC}$  of 12.2 mA cm<sup>-2</sup> and a FF of 60.6% for an active layer thickness of 30 nm. The reduction of the active layer thickness to 20 nm leads to a slightly lower PCE of 6.7%. With decreasing or increasing the length of the alkyl side chains, a reduction of the  $J_{SC}$  as well as a slight increase in series resistance ( $R_s$ ) was observed. In general, it has to be noted that the strong absorption of  $S,N$ -heterohexacenes **1-5** in the spectral range from 500 to 700 nm resulted in extremely high external quantum efficiencies (EQE), in particular higher than 80% for pentyl derivative **3** (Figure 6b). The  $J_{SC}$  values obtained from the integration of the EQE spectra (between 9.9 to 11.3 mA cm<sup>-2</sup>) were in reasonable agreement with those measured

from the  $J$ - $V$  curve. All compounds showed high saturation values of 1.04 to 1.10 exhibiting a weak voltage bias dependence of the current in the reverse direction.

**Table 4.** Photovoltaic data of BHJ solar cells of DCV-substituted heterohexacenes **1-5**: C<sub>60</sub> (2:1) at a substrate temperature of 90 °C.

Donor	D:A ratio	absorber thickness [nm]	V <sub>OC</sub> [V]	FF	J <sub>SC</sub> [mA cm <sup>-2</sup> ]	PCE [%]	R <sub>s</sub> [Ω cm <sup>2</sup> ]	Sat. <sup>a</sup>
<b>1</b>	2:1	20	0.90	60.8	10.7	<b>5.9</b>	4.54	1.07
<b>1</b>	2:1	30	0.90	58.7	10.5	<b>5.5</b>	4.39	1.09
<b>2</b>	2:1	20	0.95	62.1	10.0	<b>5.9</b>	3.86	1.07
<b>2</b>	2:1	30	0.94	55.6	10.5	<b>5.5</b>	4.11	1.09
<b>3</b>	2:1	20	0.96	63.2	11.1	<b>6.7</b>	3.51	1.10
<b>3</b>	2:1	30	0.96	60.6	12.2	<b>7.1</b>	3.77	1.04
<b>4</b>	2:1	20	0.96	60.1	10.3	<b>5.9</b>	4.62	1.06
<b>4</b>	2:1	30	0.95	54.9	11.0	<b>5.7</b>	4.29	1.07
<b>5</b>	2:1	20	0.97	62.0	11.0	<b>6.6</b>	4.24	1.05
<b>5</b>	2:1	30	0.96	57.4	11.4	<b>6.3</b>	4.48	1.06

<sup>a</sup> Defined as  $J(-1V)/J_{SC}$

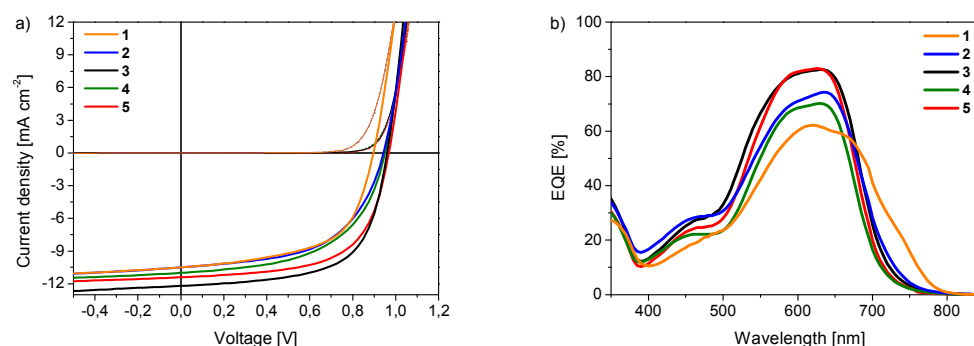


**Figure 6.**  $J$ - $V$  characteristics (a) and external quantum efficiency (EQE) spectra (b) of the optimized BHJ solar cells prepared with **1-5** as donor and C<sub>60</sub> as acceptor (active layer thickness 30 nm).

Another interesting comparison is the development of solar cell parameters in dependence of the side chain length, as it gives insight in the effect of morphological changes induced by alkyl chain length variation (Figure 7). In particular, the devices with 30 nm thickness of the active layer showed an odd-even dependency of the alkyl side chain length on PCE and  $J_{SC}$  with higher values for the odd-numbered alkyl chains, except for propyl derivative **1**. This odd-even effect was most obvious for the FF of the 30 nm blends.

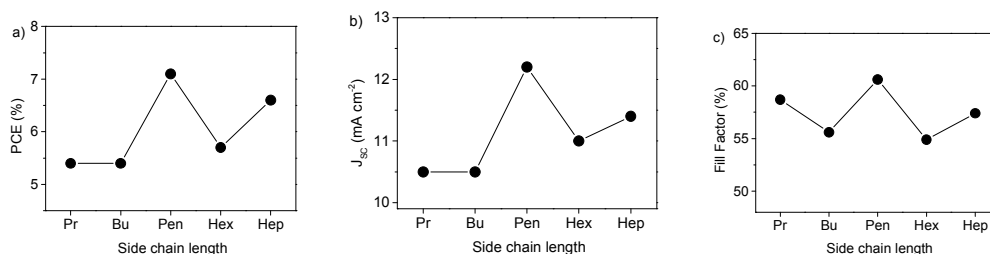


**Figure 7.** Variation of photovoltaic parameters (PCE,  $J_{sc}$ , fill factor) versus alkyl side chain length for devices with an active layer thickness of 30 nm.

The surface morphology of blends of DCV-SN6: $C_{60}$  (2:1, 30 nm) deposited onto an ITO/ $C_{60}$  surface was investigated by atomic force microscopy (AFM). Two distinct morphologies were found: as a representative, Figure 8 (top) shows the surface characterization of a 30 nm thick *S,N*-heterohexacene **1**: $C_{60}$  photoactive layer. Large crystallized domains composed by uniform structures of 80-180 nm in diameter at an average height of 30 nm were found for propyl derivative **1** in the blend (Figure 8 a,b). The corresponding phase images evidenced a very moderate shift-contrast which is indicative of a unique component or a well-mixed blend layer on the surface (Figure 8c). The larger nanostructures can at least in part explain the losses in  $V_{OC}$  observed for the BHJ solar cells. On the contrary, the **5**: $C_{60}$  photoactive blend layer revealed a uniform surface of very thin grain-like structures of 10-20 nm in diameter and 2 nm in height, apart from few big aggregates (Figure 8 d,e). The phase images showed a big phase shift of  $90^\circ$  and the histogram analysis over several phase images disclosed two well differentiated peaks, which we attribute to crystalline homophases.<sup>54-56</sup> The analysis revealed 8-15 nm large islands of the donor phase surrounded by an interconnected network of the acceptor (Figure 8f, bright and dark features, respectively) which accounts for a good phase separation and correlates with the higher performance of the corresponding photovoltaic device.

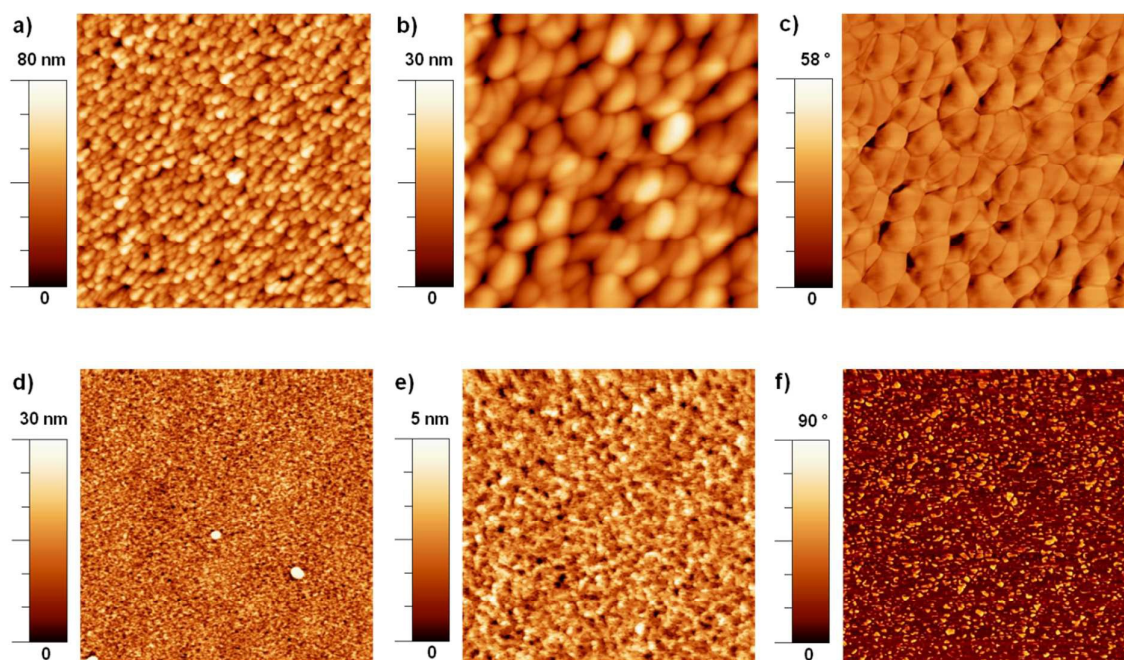


**Figure 8.** Tapping mode AFM topography (a) and d)  $5 \times 5 \mu\text{m}^2$ , b) and e)  $2 \times 2 \mu\text{m}^2$ ) and corresponding phase images (c) and f)  $2 \times 2 \mu\text{m}^2$ ) of blend films (2:1 w/w deposited at  $90^\circ\text{C}$  substrate temperature) of **1**: $\text{C}_{60}$  (top) and **5**: $\text{C}_{60}$  (bottom).

## Conclusion

In summary, we have designed and synthesized a new family of A-D-A oligomers **1-5** composed of *S,N*-heterohexacene as a planarized electron-rich donor backbone and 1,1-dicyanovinyl (DCV) as acceptor moieties for application in organic solar cells. Single crystal X-ray structure analysis of hexyl derivative **4** gave further insight into the molecular ordering by providing intermolecular N-H and N-S non-bonding interactions and good  $\pi$ - $\pi$ -stacking for efficient charge transport. The acceptor-substituted *S,N*-heterohexacenes showed high optical absorptivity and excellent thermal stability which made them suitable for vacuum-processed solar cells. The optical and electrochemical properties of the oligomers were not affected by the length of the alkyl side chains, while a noticeable influence was observed on the photovoltaic parameters. The excellent efficiency of 5.0% obtained for propyl derivative **1** represents one of the highest values ever reported for planar-heterojunction solar cells. In vacuum-processed bulk-heterojunction solar cells, all derivatives **1-5** showed high open-circuit voltages resulting in good efficiencies of around 6.0% with the highest efficiency of 7.1% for pentyl derivative **3**.

## Experimental Section

*Instrument and Measurements:* NMR spectra were recorded on a Bruker AMX 500 ( $^1\text{H}$  NMR: 500 MHz,  $^{13}\text{C}$  NMR: 125 MHz) or an Avance 400 spectrometer ( $^1\text{H}$  NMR: 400 MHz,  $^{13}\text{C}$  NMR: 100 MHz). Chemical shift values ( $\delta$ ) are expressed in parts per million using residual solvent protons ( $^1\text{H}$  NMR:  $\delta_{\text{H}} = 3.58$  for THF[ $\text{D}_8$ ];  $\delta_{\text{H}} = 5.93$  for  $\text{C}_2\text{D}_2\text{Cl}_4$ ;  $^{13}\text{C}$  NMR:  $\delta_{\text{C}} = 67.21$  for THF[ $\text{D}_8$ ];  $\delta_{\text{C}} = 74.20$  for  $\text{C}_2\text{D}_2\text{Cl}_4$ ) as internal standard. The splitting patterns are designated as follows: s (singlet), d (doublet), t (triplet) and m (multiplet). The assignments are Th- $\alpha$ -H (thiophene protons in  $\alpha$ -position), Th- $\beta$ -H (thiophene protons in  $\beta$ -position), CHO (aldehyde protons), and DCVH (dicyanovinylene protons). Elemental analyses were performed on an Elementar Vario EL. Melting points were determined using a Mettler Toledo DSC 823. Thin layer chromatography was carried out on aluminum plates, pre-coated with silica gel, Merck Si60 F254. Preparative column chromatography was performed on glass columns packed with silica gel, Merck Silica 60, particle size 40–63  $\mu\text{m}$ . High resolution MALDI mass spectra (HRMS) experiments were recorded on a MS Bruker Reflex 2 (Bruker Daltonik GmbH, Bremen, Germany), MALDI-TOF mass spectra on a Bruker Daltonics Reflex III, using *trans*-2-[3-(4-*tert*-butylphenyl)-2-methyl-2-propenylidene]malonitrile (DCTB) as matrix. Chemical ionisation (CI) mass spectra were performed on a Finnigan MAT SSQ-7000. UV-Vis absorption spectra were recorded on a Perkin Elmer Lambda 19 spectrometer. Cyclic voltammetry experiments were performed with a computer-controlled Autolab PGSTAT30 potentiostat in a three-electrode single-compartment cell with a platinum working electrode, a platinum wire counter electrode, and a Ag/AgCl reference electrode. All potentials were internally referenced to the ferrocene/ferricenium couple. Surface images of the photoactive layers were recorded with a Bruker MultiMode V AFM with Nanoscope controller at ambient temperature in tapping mode. The images were analyzed using the WSxM software.<sup>57</sup> X-ray diffraction data of a blue single crystal of DCV-SN6 **4** was collected in a stream of nitrogen at 180 K on a Agilent SuperNova, Cu at zero, Atlas CCD using graphite-monochromated Cu K $\alpha$  radiation. Data collection strategy, data reduction, and cell refinement was performed with the CrysAlis<sup>Pro</sup> software.<sup>58</sup> An absorption correction based on the semi-empirical ‘multi-scan’ approach was performed with the ABSPACK module.<sup>58</sup> The structure was solved by direct methods with superflip.<sup>59</sup> For the final model, all non-H atoms were refined anisotropically with SHELXS.<sup>58</sup> H atoms were finally placed in calculated positions, riding the parent C atom with C-H distance constraints of 0.93 Å for aromatic H atoms, 0.96 Å for methyl H atoms and 0.97 Å for methylene H atoms, and with  $U_{\text{iso}}(\text{H}) = 1.2U_{\text{eq}}(\text{C})$  for H atoms.



*Thin Film and Device Fabrication:* Thin films and heterojunction solar cell devices were prepared by thermal vapor deposition in a Creaphys ultra-high vacuum system (Creaphys GmbH, Dresden, Germany) at a base pressure of  $<10^{-7}$  mbar. The substrates were kept at room temperature for all thin films and layers, except of the absorber layers in the bulk heterojunction devices which were deposited at 80°C or 90 °C, respectively. Thin films for absorption and emission measurements were prepared on quartz substrates; solar cells on tin-doped indium oxide (ITO) coated glass (Thin Film Devices, USA, sheet resistance of 30  $\Omega$  sq.<sup>-1</sup>). Layer thicknesses were determined during evaporation by using quartz crystal monitors. The thin films prepared for absorption and emission measurements were 30 nm thick. Thin film absorption spectra were recorded on a Shimadzu UV-2101/3101 UV-Vis spectrometer. The thin film emission spectra were recorded with an Edinburgh Instruments FSP920 fluorescence spectrometer. Bulk-heterojunction solar cells were prepared layer by layer without breaking the vacuum. The blend layer of the respective donors and C<sub>60</sub> as acceptor were made at a 2:1 ratio by mass. NDP9 (purchased from Novald GmbH, Germany) was used as 10% by mass dopant inside the hole transport material BPAPF.

*Photovoltaic Characterization:* *J-V* and *EQE* measurements were carried out in a glove box with nitrogen atmosphere which was directly attached to the vacuum system. This allows inert sample transfer without contact to air. *J-V* characteristics were measured using a source-measure unit (Keithley SMU 2400) and an AM 1.5G sun simulator (KHS Technical Lighting SC1200). The intensity was monitored with a silicon photodiode (Hamamatsu S1337), which was calibrated at Fraunhofer ISE. The mismatch between the spectrum of the sun simulator and the solar AM 1.5G spectrum was taken into account for the calculation of current density. For well-defined active solar cell areas, aperture masks (2.76 mm<sup>2</sup>) were used. Simple *EQE* measurements were carried out using the sun simulator in combination with color filters for monochromatic illumination. The illumination intensities were measured with a silicon reference diode (Hamamatsu S1337).

*Materials:* Toluene (VWR) and DMF (Merck) were dried and purified by a MB SPS-800 (MBraun). DCM and *n*-hexane were purchased from VWR and distilled prior to use. Sodium *tert*-butoxide, *n*-hexyl amine, *n*-pentyl amine, *n*-propyl amine, 1,2-dichloroethane, phosphoryl chloride, sodium bicarbonate, malonitrile, and ammonium acetate were purchased from Merck. Pd(dba)<sub>2</sub>, *n*-butyl amine, and *n*-heptyl amine were purchased from Sigma Aldrich, and 1,1'-bis(diphenylphosphino)ferrocene from Frontier Scientific. 3,6-Dibromo-2,5-bis(3-bromothiophen-2-yl)thieno[3,2-*b*]thiophene **6** was prepared according to the literature.<sup>43</sup>



*Syntheses:* General procedure for the synthesis of SN6 derivatives 7-11:

**4,9-Dihexyl-thieno[3,2-*b*]thieno[2''',3''':4'',5'']pyrrolo[2'',3'':4',5']thieno[2',3':4,5]-thieno[2,3-*d*]pyrrole (10).** 3,6-Dibromo-2,5-bis(3-bromothiophen-2-yl)thieno[3,2-*b*]thiophene **6** (500 mg, 0.81 mmol), sodium-*tert*-butoxide (1.24 g, 12.90 mmol), Pd(*dba*)<sub>2</sub> (46 mg, 0.08 mmol) and dppf (179 mg, 0.32 mmol) were stirred in dry and degassed toluene (25 mL) at room temperature. After 20 min *n*-hexyl amine (0.26 mL, 1.98 mmol) was added and the mixture was stirred at 110 °C for 18 h. Water was added to the cooled reaction mixture and the aqueous phase was extracted with ethyl ether (25 mL) and dichloromethane (2 x 25 mL). The solvents were removed under reduced pressure. The crude product was purified by column chromatography under exclusion of light (flash-silica; *n*-hexane/dichloromethane 4:1). Pure SN6 **10** was obtained as a pale yellow solid (217 mg, 0.44 mmol, 54%). Mp. (DSC) 163 °C. <sup>1</sup>H-NMR (400 MHz, THF[D<sub>8</sub>], 20 °C) δ= 7.17 (d, 2H, <sup>3</sup>*J*(H,H)= 5.3 Hz; Th-β-*H*), 7.14 (d, 2H, <sup>3</sup>*J*(H,H)= 5.3 Hz; Th-α-*H*), 4.37 (t, 4H, <sup>3</sup>*J*(H,H)= 7.1 Hz; N-CH<sub>2</sub>), 1.93–2.00 (m, 4H; N-CH<sub>2</sub>-CH<sub>2</sub>), 1.28–1.46 (m, 12H; N-(CH<sub>2</sub>)<sub>2</sub>-(CH<sub>2</sub>)<sub>3</sub>), 0.87 ppm (t, 6H, <sup>3</sup>*J*(H,H)= 7.1 Hz; N-(CH<sub>2</sub>)<sub>5</sub>-CH<sub>3</sub>). <sup>13</sup>C-NMR (100 MHz, THF[D<sub>8</sub>], 20 °C): δ= 144.85, 137.66, 123.07, 122.20, 116.54, 114.85, 111.71, 48.38, 32.25, 31.93, 27.32, 23.22, 14.15. HRMS (MALDI): *m/z* calcd. for C<sub>26</sub>H<sub>30</sub>N<sub>2</sub>S<sub>4</sub> (M<sup>+</sup>) 498.12863 found 498.12882 (δm/m= 0.38 ppm). Elemental analysis: calcd. (%) for C<sub>26</sub>H<sub>30</sub>N<sub>2</sub>S<sub>4</sub>: C 62.61, H 6.06, N 5.62, S 25.71; found C 62.83, H 5.88, N 5.51, S 25.92.

The following SN6 derivatives were prepared accordingly:

**4,9-Diheptyl-thieno[3,2-*b*]thieno[2''',3''':4'',5'']pyrrolo[2'',3'':4',5']thieno[2',3':4,5]-thieno[2,3-*d*]pyrrole (11).** 51% yield; pale yellow solid; mp. (DSC) 138 °C. <sup>1</sup>H-NMR (400 MHz, THF[D<sub>8</sub>], 20 °C) δ= 7.17 (d, 2H, <sup>3</sup>*J*(H,H)= 5.3 Hz; Th-β-*H*), 7.12 (d, 2H, <sup>3</sup>*J*(H,H)= 5.3 Hz; Th-α-*H*), 4.35 (t, 4H, <sup>3</sup>*J*(H,H)= 7.1 Hz; N-CH<sub>2</sub>), 1.92-1.99 (m, 4H; N-CH<sub>2</sub>-CH<sub>2</sub>), 1.28–1.46 (m, 16H; N-(CH<sub>2</sub>)<sub>2</sub>-(CH<sub>2</sub>)<sub>4</sub>), 0.85 ppm (t, 6H, <sup>3</sup>*J*(H,H)= 6.9 Hz; N-(CH<sub>2</sub>)<sub>6</sub>-CH<sub>3</sub>). <sup>13</sup>C-NMR (100 MHz, THF[D<sub>8</sub>], 20 °C): δ= 144.85, 137.68, 123.05, 122.21, 116.55, 114.86, 111.71, 48.39, 32.48, 31.96, 29.76, 27.63, 23.28, 14.19. MS (MALDI-TOF): *m/z* calcd. for C<sub>28</sub>H<sub>34</sub>N<sub>2</sub>S<sub>4</sub> (M<sup>+</sup>) 526.2 found 526.3. Elemental analysis: calcd. (%) for C<sub>28</sub>H<sub>34</sub>N<sub>2</sub>S<sub>4</sub>: C 63.83, H 6.50, N 5.32, S 24.35; found C 63.74, H 6.61, N 5.21, S 24.19.

**4,9-Dipentyl-thieno[3,2-*b*]thieno[2''',3''':4'',5'']pyrrolo[2'',3'':4',5']thieno[2',3':4,5]-thieno[2,3-*d*]pyrrole (9).** 62% yield; pale yellow solid; mp. (DSC) 186 °C. <sup>1</sup>H-NMR (400 MHz, THF[D<sub>8</sub>], 20 °C) δ= 7.18 (d, 2H, <sup>3</sup>*J*(H,H)= 5.3 Hz; Th-β-*H*), 7.13 (d, 2H, <sup>3</sup>*J*(H,H)= 5.3 Hz; Th-α-*H*), 4.37 (t, 4H, <sup>3</sup>*J*(H,H)= 7.1 Hz; N-CH<sub>2</sub>), 1.93–2.00 (m, 4H; N-CH<sub>2</sub>-CH<sub>2</sub>), 1.38–

1.42 (m, 8H; N-(CH<sub>2</sub>)<sub>2</sub>-(CH<sub>2</sub>)<sub>2</sub>), 0.89 ppm (t, 6H, <sup>3</sup>J(H,H)= 7.0 Hz; N-(CH<sub>2</sub>)<sub>4</sub>-CH<sub>3</sub>). <sup>13</sup>C-NMR (100 MHz, [THF[D<sub>8</sub>], 20 °C): δ= 144.83, 137.65, 123.06, 122.19, 116.53, 114.84, 111.70, 48.34, 31.67, 29.76, 23.10, 14.10. HRMS (MALDI): *m/z* calcd. for C<sub>24</sub>H<sub>26</sub>N<sub>2</sub>S<sub>4</sub> (M<sup>+</sup>) 470.09733 found 470.09742 (δ*m/m*= 0.19 ppm). Elemental analysis: calcd. (%) for C<sub>24</sub>H<sub>26</sub>N<sub>2</sub>S<sub>4</sub>: C 61.24, H 5.57, N 5.95, S 27.25; found C 61.26, H 5.37, N 5.88, S 27.09.

**4,9-Dibutyl-thieno[3,2-*b*]thieno[2''',3''':4'',5'']pyrrolo[2'',3'':4',5']thieno[2',3':4,5]-thieno[2,3-*d*]pyrrole (8).** 49% yield; pale yellow solid; mp. (DSC) 209 °C. <sup>1</sup>H-NMR (400 MHz, THF[D<sub>8</sub>], 20 °C) δ= 7.17 (d, 2H, <sup>3</sup>J(H,H)= 5.3 Hz; Th-β-*H*), 7.12 (d, 2H, <sup>3</sup>J(H,H)= 5.3 Hz; Th-α-*H*), 4.35 (t, 4H, <sup>3</sup>J(H,H)= 7.1 Hz; N-CH<sub>2</sub>), 1.89-1.96 (m, 4H; N-CH<sub>2</sub>-CH<sub>2</sub>), 1.38-1.42 (m, 4H; N-(CH<sub>2</sub>)<sub>2</sub>-CH<sub>2</sub>), 0.95 ppm (t, 6H, <sup>3</sup>J(H,H)= 7.4 Hz; N-(CH<sub>2</sub>)<sub>3</sub>-CH<sub>3</sub>). <sup>13</sup>C-NMR (100 MHz, [THF[D<sub>8</sub>], 20 °C): δ= 144.84, 137.67, 123.05, 122.21, 116.55, 114.85, 111.72, 48.11, 34.05, 20.82, 13.94. MS (CI, 100 eV): *m/z* (%): 443 (100) [M+H<sup>+</sup>] Elemental analysis: calcd. (%) for C<sub>22</sub>H<sub>22</sub>N<sub>2</sub>S<sub>4</sub>: C 59.69, H 5.01, N 6.33, S 28.97; found C 59.79, H 5.16, N 6.25, S 28.97.

**4,9-Dipropyl-thieno[3,2-*b*]thieno[2''',3''':4'',5'']pyrrolo[2'',3'':4',5']thieno[2',3':4,5]-thieno[2,3-*d*]pyrrole (7).** 74% yield; pale yellow solid; mp. (DSC) 226 °C. <sup>1</sup>H-NMR (400 MHz, THF[D<sub>8</sub>], 20 °C) δ= 7.17 (d, 2H, <sup>3</sup>J(H,H)= 5.3 Hz; Th-β-*H*), 7.13 (d, 2H, <sup>3</sup>J(H,H)= 5.3 Hz; Th-α-*H*), 4.32 (t, 4H, <sup>3</sup>J(H,H)= 7.0 Hz; N-CH<sub>2</sub>), 1.94-2.03 (m, 4H; N-CH<sub>2</sub>-CH<sub>2</sub>), 0.97 ppm (t, 6H, <sup>3</sup>J(H,H)= 7.4 Hz; N-(CH<sub>2</sub>)<sub>2</sub>-CH<sub>3</sub>). <sup>13</sup>C-NMR (100 MHz, THF[D<sub>8</sub>], 20 °C): δ= 144.91, 137.74, 123.08, 122.21, 116.53, 114.81, 111.75, 49.85, 25.16, 11.48. MS (CI, 100 eV): *m/z* (%): 414 (100) [M<sup>+</sup>]. Elemental analysis: calcd. (%) for C<sub>20</sub>H<sub>18</sub>N<sub>2</sub>S<sub>4</sub>: C 57.93, H 4.38, N 6.76, S 30.93; found C 57.87, H 4.46, N 6.64, S 30.84.

General procedure for the synthesis of dialdehydes **12-16**:

**[4,9-Dihexyl-thieno[3,2-*b*]thieno[2''',3''':4'',5'']pyrrolo[2'',3'':4',5']thieno[2',3':4,5]-thieno[2,3-*d*]pyrrole]-2,7-dicarbaldehyde (15).** A solution of *N,N*-dimethylformamide (0.53 mL, 6.90 mmol) in 1,2-dichloroethane (8 mL) was cooled down to 0 °C. Phosphoryl chloride (0.63 mL, 6.90 mmol) was added and the solution was stirred for 2 h at room temperature. Then a solution of SN6 **10** (172 mg, 0.34 mmol) in 1,2-dichloroethane (40 mL) was added dropwise. The solution was stirred at 75 °C. After 17 h the suspension was diluted with dichloromethane (800 mL). Then the solution was given to a saturated NaHCO<sub>3</sub> solution (800 mL). The mixture was stirred at room temperature until completion of the reaction which was

checked by TLC. The aqueous phase was extracted with dichloromethane (2 x 400 mL). After removing the solvent and purification by column chromatography (flash-silica; dichloromethane) dialdehyde **15** was obtained as an orange solid (185 mg, 0.33 mmol, 98%). Mp. (DSC) 319 °C. <sup>1</sup>H-NMR (500 MHz, TCE[D<sub>2</sub>], 83 °C) δ= 9.84 (s, 2H; CHO), 7.61 (s, 2H; Th-β-H), 4.30 (t, 4H, <sup>3</sup>J(H,H)= 7.3 Hz; N-CH<sub>2</sub>), 1.96-2.01 (m, 4H; N-CH<sub>2</sub>-CH<sub>2</sub>), 1.42-1.47 (m, 4H; N-(CH<sub>2</sub>)<sub>2</sub>-CH<sub>2</sub>), 1.30-1.39 (m, 8H; N-(CH<sub>2</sub>)<sub>3</sub>-(CH<sub>2</sub>)<sub>2</sub>), 0.88 ppm (t, 6H, <sup>3</sup>J(H,H)= 7.1 Hz; N-(CH<sub>2</sub>)<sub>5</sub>-CH<sub>3</sub>). <sup>13</sup>C-NMR (125 MHz, TCE[D<sub>2</sub>], 84 °C): δ= 182.46, 144.28, 141.45, 141.18, 124.73, 124.44, 118.82, 116.85, 48.61, 31.49, 31.18, 26.81, 22.56, 13.96. HRMS (MALDI): *m/z* calcd. for C<sub>28</sub>H<sub>30</sub>N<sub>2</sub>O<sub>2</sub>S<sub>4</sub> (M<sup>+</sup>) 554.11846 found 554.11814 (δ*m/m*= 0.58 ppm). Elemental analysis: calcd. (%) for C<sub>28</sub>H<sub>30</sub>N<sub>2</sub>O<sub>2</sub>S<sub>4</sub>: C 60.62, H 5.45, N 5.05, S 23.12; found: C 60.43, H 5.48, N 4.94, S 23.09.

The following dialdehydes were prepared accordingly:

**[4,9-Diheptyl-thieno[3,2-*b*]thieno[2''',3''':4'',5'']pyrrolo[2'',3'':4',5']thieno[2',3':4,5]thieno-[2,3-*d*]pyrrole]-2,7-dicarbaldehyde (16)**. 98% yield; orange solid; mp. (DSC) 266 °C. <sup>1</sup>H-NMR (400 MHz, TCE[D<sub>2</sub>], 20 °C) δ= 9.72 (s, 2H; CHO), 7.49 (s, 2H; Th-β-H), 4.20 (t, 4H, <sup>3</sup>J(H,H)= 7.1 Hz; N-CH<sub>2</sub>), 1.83-1.90 (m, 4H; N-CH<sub>2</sub>-CH<sub>2</sub>), 1.18-1.34 (m, 16H; N-(CH<sub>2</sub>)<sub>2</sub>-(CH<sub>2</sub>)<sub>4</sub>), 0.79 ppm (t, 6H, <sup>3</sup>J(H,H)= 6.9 Hz; N-(CH<sub>2</sub>)<sub>6</sub>-CH<sub>3</sub>). <sup>13</sup>C-NMR (100 MHz, TCE[D<sub>2</sub>], 20 °C): δ= 183.19, 143.93, 141.17, 140.48, 124.35, 123.98, 119.99, 116.48, 48.58, 31.90, 31.42, 29.20, 27.25, 22.90, 14.47. HRMS (MALDI): *m/z* calcd. for C<sub>30</sub>H<sub>34</sub>N<sub>2</sub>O<sub>2</sub>S<sub>4</sub> (M<sup>+</sup>) 582.14976 found 582.14992 (δ*m/m*= 0.27 ppm). Elemental analysis: calcd. (%) for C<sub>30</sub>H<sub>34</sub>N<sub>2</sub>O<sub>2</sub>S<sub>4</sub>: C 61.82, H 5.88, N 4.81, S 22.01; found: C 62.07, H 5.67, N 4.68, S 21.97.

**[4,9-Dipentyl-thieno[3,2-*b*]thieno[2''',3''':4'',5'']pyrrolo[2'',3'':4',5']thieno[2',3':4,5]thieno-[2,3-*d*]pyrrole]-2,7-dicarbaldehyde (14)**. 89% yield; orange solid; mp. (DSC) 355 °C. <sup>1</sup>H-NMR (500 MHz, TCE[D<sub>2</sub>], 85 °C) δ= 9.84 (s, 2H; CHO), 7.61 (s, 2H; Th-β-H), 4.30 (t, 4H, <sup>3</sup>J(H,H)= 7.2 Hz; N-CH<sub>2</sub>), 1.97-2.01 (m, 4H; N-CH<sub>2</sub>-CH<sub>2</sub>), 1.39-1.45 (m, 8H; N-(CH<sub>2</sub>)<sub>2</sub>-(CH<sub>2</sub>)<sub>2</sub>), 0.92 ppm (t, 6H, <sup>3</sup>J(H,H)= 6.9 Hz; N-(CH<sub>2</sub>)<sub>4</sub>-CH<sub>3</sub>). <sup>13</sup>C-NMR (125 MHz, TCE[D<sub>2</sub>], 87 °C): δ= 182.45, 144.29, 141.45, 141.21, 124.75, 124.45, 118.77, 116.86, 48.59, 30.88, 29.28, 22.40, 13.92. HRMS (LDI): *m/z* calcd. for C<sub>26</sub>H<sub>26</sub>N<sub>2</sub>O<sub>2</sub>S<sub>4</sub> (M<sup>+</sup>) 526.08716 found 526.08710 (δ*m/m*= 0.11 ppm). Elemental analysis: calcd. (%) for C<sub>26</sub>H<sub>26</sub>N<sub>2</sub>O<sub>2</sub>S<sub>4</sub>: C 59.28, H 4.98, N 5.32, S 24.35; found: C 59.45, H 4.96, N 5.36, S 24.16.

**[4,9-Dibutyl-thieno[3,2-*b*]thieno[2''',3''':4'',5'']pyrrolo[2'',3'':4',5']thieno[2',3':4,5]thieno[2,3-*d*]pyrrole]-2,7-dicarbaldehyde (13).** 86% yield; orange solid; mp. (DSC) 340 °C. <sup>1</sup>H-NMR (500 MHz, TCE[D<sub>2</sub>], 86 °C) δ= 9.85 (s, 2H; CHO), 7.61 (s, 2H; Th-β-H), 4.32 (t, 4H, <sup>3</sup>J(H,H)= 7.2 Hz; N-CH<sub>2</sub>), 1.95-2.01 (m, 4H; N-CH<sub>2</sub>-CH<sub>2</sub>), 1.44-1.51 (m, 4H; N-(CH<sub>2</sub>)<sub>2</sub>-CH<sub>2</sub>), 1.00 ppm (t, 6H, <sup>3</sup>J(H,H)= 7.4 Hz; N-(CH<sub>2</sub>)<sub>3</sub>-CH<sub>3</sub>). <sup>13</sup>C-NMR (125 MHz, TCE[D<sub>2</sub>], 87 °C): δ= 182.46, 144.30, 141.47, 141.23, 124.76, 124.47, 118.77, 116.86, 48.32, 33.28, 20.42, 13.78. MS (MALDI-TOF): *m/z* calcd. for C<sub>24</sub>H<sub>22</sub>N<sub>2</sub>O<sub>2</sub>S<sub>4</sub> (M<sup>+</sup>) 498.0 found 498.0. Elemental analysis: calcd. (%) for C<sub>24</sub>H<sub>22</sub>N<sub>2</sub>O<sub>2</sub>S<sub>4</sub>: C 57.80, H 4.45, N 5.62, S 25.72; found: C 57.55, H 4.48, N 5.43, S 25.72.

**[4,9-Dipropyl-thieno[3,2-*b*]thieno[2''',3''':4'',5'']pyrrolo[2'',3'':4',5']thieno[2',3':4,5]-thieno[2,3-*d*]pyrrole]-2,7-dicarbaldehyde (12).** 92% yield; orange solid; mp. (DSC) 361 °C. <sup>1</sup>H-NMR (400 MHz, TCE[D<sub>2</sub>], 20 °C) δ= 9.78 (s, 2H; CHO), 7.61 (s, 2H; Th-β-H), 4.25 (t, 4H, <sup>3</sup>J(H,H)= 6.9 Hz; N-CH<sub>2</sub>), 1.90-1.99 (m, 4H; N-CH<sub>2</sub>-CH<sub>2</sub>), 0.96 ppm (t, 6H, <sup>3</sup>J(H,H)= 7.3 Hz; N-(CH<sub>2</sub>)<sub>2</sub>-CH<sub>3</sub>). <sup>13</sup>C-NMR could not be measured due to low solubility. HRMS (MALDI): *m/z* calcd. for C<sub>22</sub>H<sub>18</sub>N<sub>2</sub>O<sub>2</sub>S<sub>4</sub> (M<sup>+</sup>) 470.02456 found 470.02406 (δm/m = 1.06 ppm).

General procedure for the synthesis of DCV end-capped SN6 derivatives **1-5**:

**[4,9-Dihexyl-thieno[3,2-*b*]thieno[2''',3''':4'',5'']pyrrolo[2'',3'':4',5']thieno[2',3':4,5]-thieno[2,3-*d*]pyrrole]-2,8-bis[methan-1-yl-1-yliden]dimalonodinitrile (4).** Dialdehyde **15** (185 mg, 0.33 mmol), malonodinitrile (500 mg, 7.56 mmol), and ammonium acetate (500 mg, 6.49 mmol) were dissolved in 1,2-dichloroethane (300 mL) and the reaction mixture was heated at 80 °C. After 48 h a large excess of malonodinitrile and ammonium acetate were added and the reaction was continued until completion of the reaction which was checked by TLC. After 7 days the mixture was allowed to cool down to room temperature. The resulting solid was filtered off and thoroughly washed with hot methanol. The oligomer **4** was obtained as a blue solid (193 mg, 0.30 mmol, 89%). The compound was further purified by gradient vacuum sublimation. Mp. (DSC) 373 °C. <sup>1</sup>H-NMR (500 MHz, TCE[D<sub>2</sub>], 87 °C) δ= 7.70 (s, 2H; DCVH), 7.65 (s, 2H; Th-β-H), 4.31 (t, 4H, <sup>3</sup>J(H,H)= 7.1 Hz; N-CH<sub>2</sub>), 1.96-2.01 (m, 4H; N-CH<sub>2</sub>-CH<sub>2</sub>), 1.32-1.47 (m, 12H; N-(CH<sub>2</sub>)<sub>2</sub>-(CH<sub>2</sub>)<sub>3</sub>), 0.88 ppm (t, 6H, <sup>3</sup>J(H,H)= 7.1 Hz; N-(CH<sub>2</sub>)<sub>5</sub>-CH<sub>3</sub>). <sup>13</sup>C-NMR could not be measured due to low solubility. HRMS (LDI): *m/z* calcd. for C<sub>34</sub>H<sub>30</sub>N<sub>6</sub>S<sub>4</sub> (M<sup>+</sup>) 650.14093 found 650.14102 (δm/m = 0.14 ppm).

The following DCV end-capped SN6 derivatives were prepared accordingly:

**[4,9-Diheptyl-thieno[3,2-*b*]thieno[2''',3''':4'',5'']pyrrolo[2'',3'':4',5']thieno[2',3':4,5]-thieno[2,3-*d*]pyrrole]-2,8-bis[methan-1-yl-1-yliden]dimalonodinitrile (5).** 93% yield; blue solid; mp. (DSC) 366 °C. <sup>1</sup>H-NMR (500 MHz, TCE[D<sub>2</sub>], 86 °C) δ= 7.70 (s, 2H; DCVH), 7.65 (s, 2H; Th-β-*H*), 4.31 (t, 4H, <sup>3</sup>*J*(H,H)= 7.2 Hz; N-CH<sub>2</sub>), 1.96-2.01 (m, 4H; N-CH<sub>2</sub>-CH<sub>2</sub>), 1.28-1.47 (m, 16H; N-(CH<sub>2</sub>)<sub>2</sub>-(CH<sub>2</sub>)<sub>4</sub>), 0.87 ppm (t, 6H, <sup>3</sup>*J*(H,H)= 7.0 Hz; N-(CH<sub>2</sub>)<sub>6</sub>-CH<sub>3</sub>). <sup>13</sup>C-NMR could not be measured due to low solubility. HRMS (LDI): *m/z* calcd. for C<sub>36</sub>H<sub>34</sub>N<sub>6</sub>S<sub>4</sub> (M<sup>+</sup>) 678.17223 found 678.17191 (δ*m/m* = 0.47 ppm).

**[4,9-Dipentyl-thieno[3,2-*b*]thieno[2''',3''':4'',5'']pyrrolo[2'',3'':4',5']thieno[2',3':4,5]-thieno[2,3-*d*]pyrrole]-2,8-bis[methan-1-yl-1-yliden]dimalonodinitrile (3).** 96% yield; blue solid; mp. (DSC) 411 °C. <sup>1</sup>H-NMR (400 MHz, TCE[D<sub>2</sub>], 87 °C) δ= 7.70 (s, 2H; DCVH), 7.65 (s, 2H; Th-β-*H*), 4.32 (t, 4H, <sup>3</sup>*J*(H,H)= 7.1 Hz; N-CH<sub>2</sub>), 1.97-2.03 (m, 4H; N-CH<sub>2</sub>-CH<sub>2</sub>), 1.38-1.44 (m, 8H; N-(CH<sub>2</sub>)<sub>2</sub>-(CH<sub>2</sub>)<sub>2</sub>), 0.93 ppm (t, 6H, <sup>3</sup>*J*(H,H)= 6.8 Hz; N-(CH<sub>2</sub>)<sub>4</sub>-CH<sub>3</sub>). <sup>13</sup>C-NMR could not be measured due to low solubility. HRMS (LDI): *m/z* calcd. For C<sub>32</sub>H<sub>26</sub>N<sub>6</sub>S<sub>4</sub> (M<sup>+</sup>) 622.10963 found 622.11011 (δ*m/m* = 0.77 ppm).

**[4,9-Dibutyl-thieno[3,2-*b*]thieno[2''',3''':4'',5'']pyrrolo[2'',3'':4',5']thieno[2',3':4,5]-thieno[2,3-*d*]pyrrole]-2,8-bis[methan-1-yl-1-yliden]dimalonodinitrile (2).** 92% yield; blue solid; mp. (DSC) 427 °C. <sup>1</sup>H-NMR (400 MHz, TCE[D<sub>2</sub>], 87 °C) δ= 7.70 (s, 2H; DCVH), 7.67 (s, 2H; Th-β-*H*), 4.33 (t, 4H, <sup>3</sup>*J*(H,H)= 7.1 Hz; N-CH<sub>2</sub>), 1.95-2.01 (m, 4H; N-CH<sub>2</sub>-CH<sub>2</sub>), 1.45-1.51 (m, 4H; N-(CH<sub>2</sub>)<sub>2</sub>-CH<sub>2</sub>), 1.01 ppm (t, 6H, <sup>3</sup>*J*(H,H)= 6.8 Hz; N-(CH<sub>2</sub>)<sub>3</sub>-CH<sub>3</sub>). <sup>13</sup>C-NMR could not be measured due to low solubility. HRMS (LDI): *m/z* calcd. for C<sub>30</sub>H<sub>22</sub>N<sub>6</sub>S<sub>4</sub> (M<sup>+</sup>) 594.07833 found 594.07804 (δ*m/m* = 0.49 ppm).

**[4,9-Dipropyl-thieno[3,2-*b*]thieno[2''',3''':4'',5'']pyrrolo[2'',3'':4',5']thieno[2',3':4,5]-thieno[2,3-*d*]pyrrole]-2,8-bis[methan-1-yl-1-yliden]dimalonodinitrile (1).** 89% yield; blue solid; mp. (DSC) 468 °C. Both <sup>1</sup>H-NMR and <sup>13</sup>C-NMR could not be measured due to low solubility. HRMS (LDI): *m/z* calcd. for C<sub>28</sub>H<sub>18</sub>N<sub>6</sub>S<sub>4</sub> (M<sup>+</sup>) 566.04703 found 566.04678 (δ*m/m* = 0.44 ppm).

*X-Ray crystal structure analysis:*

DCV-SN6 4 (CCDC number: 1433672)

Bond precision: C-C = 0.0022 Å  
Cell: a=4.94184(3) b=32.8876(2)

Wavelength=1.54184  
c=19.72071(13)

alpha=90	beta=96.1585(6)	gamma=90
Temperature: 180 K		
	Calculated	Reported
Volume	3186.62(3)	3186.62(4)
Space group	P 21/c	P 1 21/c 1
Hall group	-P 2ybc	-P 2ybc
Moiety formula	C34 H30 N6 S4	C34 H30 N6 S4
Sum formula	C34 H30 N6 S4	C34 H30 N6 S4
Mr	650.88	650.88
Dx, g cm <sup>-3</sup>	1.357	1.357
Z	4	4
Mu (mm <sup>-1</sup> )	3.012	3.012
F000	1360.0	1360.0
F000'	1368.33	
h,k,lmax	6,41,24	6,41,24
Nref	6695	6665
Tmin,Tmax	0.704,0.835	0.882,0.957
Tmin'	0.568	
Correction method= # Reported		T Limits: Tmin=0.882 Tmax=0.957
AbsCorr = GAUSSIAN		
Data completeness= 0.996		Theta(max)= 76.487
R(reflections)= 0.0341( 6430)		wR2(reflections)= 0.0872( 6665)
S = 1.069		Npar= 425

### Acknowledgements

The authors thank the German Federal Ministry of Education and Research (BMBF, program LOTsE 03EK3505G) for financial support.

### References

- 1 C. Z. Li, C. Y. Chang, Y. Zang, H. X. Ju, C. C. Chueh, P. W. Liang, N. Cho, D. S. Ginger and A. K. Y. Jen, *Adv. Mater.*, 2014, **26**, 6262–6267.
- 2 L. Huo, T. Liu, X. Sun, Y. Cai, A. J. Heeger and Y. Sun, *Adv. Mater.*, 2015, **27**, 2938–2944.
- 3 K. Sun, Z. Xiao, S. Lu, W. Zajaczkowski, W. Pisula, E. Hanssen, J. M. White, R. M. Williamson, J. Subbiah, J. Ouyang, A. B. Holmes, W. W. H. Wong and D. J. Jones, *Nat. Commun.*, 2015, **6**, 6013.
- 4 B. Kan, Q. Zhang, M. Li, X. Wan, W. Ni, G. Long, Y. Wang, X. Yang, H. Feng and Y. Chen, *J. Am. Chem. Soc.*, 2014, **136**, 15529–15532.
- 5 B. Kan, M. Li, Q. Zhang, F. Liu, X. Wan, Y. Wang, W. Ni, G. Long, X. Yang, H. Feng, Y. Zuo, M. Zhang, F. Huang, Y. Cao, T. P. Russell and Y. Chen, *J. Am. Chem. Soc.*, 2015, **137**, 3886–3893.

- 6 W. Li, A. Furlan, K. H. Hendriks, M. M. Wienk and R. A. J. Janssen, *J. Am. Chem. Soc.*, 2013, **135**, 5529–5532.
- 7 J. You, C. C. Chen, Z. Hong, K. Yoshimura, K. Ohya, R. Xu, S. Ye, J. Gao, G. Li and Y. Yang, *Adv. Mater.*, 2013, **25**, 3973–3978.
- 8 J. You, L. Dou, K. Yoshimura, T. Kato, K. Ohya, T. Moriarty, K. Emery, C.-C. Chen, J. Gao, G. Li and Y. Yang, *Nat. Commun.*, 2013, **4**, 1446.
- 9 Y. Liu, C.-C. Chen, Z. Hong, J. Gao, Y. M. Yang, H. Zhou, L. Dou, G. Li and Y. Yang, *Sci. Rep.*, 2013, **3**, 3356 Doi:3310.1038/srep03356.
- 10 H. Zhou, Y. Zhang, C.-K. Mai, S. D. Collins, G. C. Bazan, T.-Q. Nguyen and A. J. Heeger, *Adv. Mater.*, 2015, **27**, 1767–1773.
- 11 H. Zhou, L. Yang and W. You, *Macromolecules*, 2012, **45**, 607–632.
- 12 R. Po, G. Bianchi, C. Carbonera and A. Pellegrino, *Macromolecules*, 2015, **48**, 453–461.
- 13 A. Mishra and P. Bäuerle, *Angew. Chem. Int. Ed.*, 2012, **51**, 2020–2067.
- 14 Y. Liu, J. Zhao, Z. Li, C. Mu, W. Ma, H. Hu, K. Jiang, H. Lin, H. Ade and H. Yan, *Nat. Commun.*, 2014, **5**, 5293.
- 15 J. A. Love, I. Nagao, Y. Huang, M. Kuik, V. Gupta, C. J. Takacs, J. E. Coughlin, L. Qi, T. S. Van Der Poll, E. J. Kramer, A. J. Heeger, T. Q. Nguyen and G. C. Bazan, *J. Am. Chem. Soc.*, 2014, **136**, 3597–3606.
- 16 J. A. Love, S. D. Collins, I. Nagao, S. Mukherjee, H. Ade, G. C. Bazan and T.-Q. Nguyen, *Adv. Mater.*, 2014, **26**, 7308–7316.
- 17 C. D. Wessendorf, G. L. Schulz, A. Mishra, P. Kar, I. Ata, M. Weidener, M. Urdanpilleta, J. Hanisch, E. Mena-Osteritz, M. Lindén, E. Ahlswede and P. Bäuerle, *Adv. Energy Mater.*, 2014, **4**, 1400266.
- 18 K. Schulze, C. Urich, R. Schüppel, K. Leo, M. Pfeiffer, E. Brier, E. Reinold and P. Bäuerle, *Adv. Mater.*, 2006, **18**, 2872–2875.
- 19 K. Cnops, B. P. Rand, D. Cheyons, B. Verreert, M. A. Empl and P. Heremans, *Nat. Commun.*, 2014, **5**, 3406.
- 20 F. Würthner and K. Meerholz, *Chem. Eur. J.*, 2010, **16**, 9366–9373.
- 21 N. M. Kronenberg, V. Steinmann, H. Bürckstümmer, J. Hwang, D. Hertel, F. Würthner and K. Meerholz, *Adv. Mater.*, 2010, **22**, 4193–4197.
- 22 Y. Chen, L. Lin, C. Lu, F. Lin, Z. Huang, H. Lin, P. Wang, Y. Liu, K. Wong, J. Wen, D. J. Miller and S. B. Darling, *J. Am. Chem. Soc.*, 2012, **134**, 13616–13623.

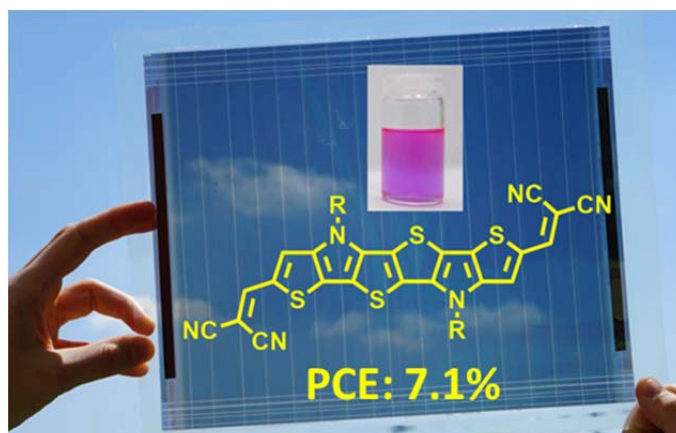


- 23 Y. Zou, J. Holst, Y. Zhang and R. J. Holmes, *J. Mater. Chem. A*, 2014, **2**, 12397–12402.
- 24 R. Fitzner, E. Mena-Osteritz, K. Walzer, M. Pfeiffer and P. Bäuerle, *Adv. Funct. Mater.*, 2015, **25**, 1845–1856.
- 25 M. Löbert, A. Mishra, C. Uhrich, M. Pfeiffer and P. Bäuerle, *J. Mat. Chem. C*, 2014, **2**, 4879–4892.
- 26 R. Fitzner, E. Mena-Osteritz, A. Mishra, G. Schulz, E. Reinold, M. Weil, C. Körner, H. Ziehlke, C. Elschner, K. Leo, M. Riede, M. Pfeiffer, C. Uhrich and P. Bäuerle, *J. Am. Chem. Soc.*, 2012, **134**, 11064–11067.
- 27 R. Fitzner, E. Reinold, A. Mishra, E. Mena-Osteritz, H. Ziehlke, C. Körner, K. Leo, M. Riede, M. Weil, O. Tsaryova, A. Weiß, C. Uhrich, M. Pfeiffer and P. Bäuerle, *Adv. Funct. Mater.*, 2011, **21**, 897–910.
- 28 A. Mishra, C. Uhrich, E. Reinold, M. Pfeiffer and P. Bäuerle, *Adv. Energy Mat.*, 2011, **1**, 265–273.
- 29 S. Steinberger, A. Mishra, G. Schulz, C. Uhrich, M. Pfeiffer and P. Bäuerle, *Org. Photonics Photovolt.*, 2014, **2**, 40–49.
- 30 S. Haid, A. Mishra, M. Weil, C. Uhrich, M. Pfeiffer and P. Bäuerle, *Adv. Funct. Mater.*, 2012, **22**, 4322–4333.
- 31 S. Steinberger, A. Mishra, E. Reinold, E. Mena-Osteritz, H. Müller, C. Uhrich, M. Pfeiffer and P. Bäuerle, *J. Mater. Chem.*, 2012, **22**, 2701.
- 32 S. Haid, A. Mishra, C. Uhrich, M. Pfei and B. Peter, *Chem Mater.*, 2011, 4435–4444.
- 33 S. Steinberger, A. Mishra, E. Reinold, C. M. Müller, C. Uhrich, M. Pfeiffer and P. Bäuerle, *Org. Lett.*, 2011, **13**, 90–93.
- 34 R. Meerheim, C. Körner and K. Leo, *Appl. Phys. Lett.*, 2014, **105**, 063306.
- 35 <http://www.heliatek.com> and <http://www.uni-ulm.de/nawi/nawi-oc2>, accessed February 18th, 2014.
- 36 X. Che, X. Xiao, J. D. Zimmerman, D. Fan and S. R. Forrest, *Adv. Energy Mat*, 2014, **4**, 1400568.
- 37 C. Wetzel, E. Brier, A. Vogt, A. Mishra, E. Mena-Osteritz and P. Bäuerle, *Angew. Chem. Int. Ed.*, 2015, **54**, 12334–12338.
- 38 A. Mishra, D. Popovic, A. Vogt, H. Kast, T. Leitner, K. Walzer, M. Pfeiffer, E. Mena-Osteritz and P. Bäuerle, *Adv. Mater.*, 2014, **26**, 7217–7223.
- 39 H. Kast, A. Mishra, G. L. Schulz, M. Urdanpilleta, E. Mena-Osteritz and P. Bäuerle, *Adv. Funct. Mater.*, 2015, **15**, 3414–3424.

- 40 P. Qin, H. Kast, M. K. Nazeeruddin, S. K. Zakeeruddin, A. Mishra, P. Bäuerle and M. Grätzel, *Energy Environ. Sci.*, 2014, **7**, 2981–2985.
- 41 C. Steck, M. Franckevičius, S. M. Zakeeruddin, A. Mishra, P. Bäuerle and M. Grätzel, *J. Mater. Chem. A*, 2015, **3**, 17738–17746.
- 42 D. Bi, A. Mishra, P. Gao, M. Franckevičius, C. Steck, S. M. Zakeeruddin, M. K. Nazeeruddin, P. Bäuerle, M. Grätzel and A. Hagfeldt, *Adv. Mater.* (submitted).
- 43 C. Wetzel, A. Mishra, E. Mena-Osteritz, A. Liess, M. Stolte, F. Würthner and P. Bäuerle, *Org. Lett.*, 2014, **16**, 362–365.
- 44 C.-L. Chung, C.-Y. Chen, H.-W. Kang, H.-W. Lin, W.-L. Tsai, C.-C. Hsu and K.-T. Wong, *Org. Electron.*, 2016, **28**, 229–238.
- 45 H. Minemawari, T. Yamada, H. Matsui, J. Tsutsumi, S. Haas, R. Chiba, R. Kumai and T. Hasegawa, *Nature*, 2011, **475**, 364–368.
- 46 A. Y. Amin, A. Khassanov, K. Reuter, T. Meyer-Friedrichsen and M. Halik, *J. Am. Chem. Soc.*, 2012, **134**, 16548–16550.
- 47 H. Bronstein, Z. Chen, R. S. Ashraf, W. Zhang, J. Du, J. R. Durrant, P. S. Tuladhar, K. Song, S. E. Watkins, Y. Geerts, M. M. Wienk, R. A. J. Janssen, T. Anthopoulos, H. Sirringhaus, M. Heeney and I. McCulloch, *J. Am. Chem. Soc.*, 2011, **133**, 3272–3275.
- 48 I. Meager, M. Nikolka, B. C. Schroeder, C. B. Nielsen, M. Planells, H. Bronstein, J. W. Rumer, D. I. James, R. S. Ashraf, A. Sadhanala, P. Hayoz, J.-C. Flores, H. Sirringhaus and I. McCulloch, *Adv. Funct. Mater.*, 2014, **24**, 7109–7115.
- 49 B. C. Schroeder, R. S. Ashraf, S. Thomas, A. J. P. White, L. Biniek, C. B. Nielsen, W. Zhang, Z. Huang, P. S. Tuladhar, S. E. Watkins, T. D. Anthopoulos, J. R. Durrant and I. McCulloch, *Chem. Commun.*, 2012, **48**, 7699–7701.
- 50 A. Yassin, T. Rousseau, P. Leriche, A. Cravino and J. Roncali, *Sol. Energy Mater. Sol. Cells*, 2011, **95**, 462–468.
- 51 L. J. A. Koster, V. D. Mihailetschi, R. Ramaker and P. W. M. Blom, *Appl. Phys. Lett.*, 2005, **86**, 123509.
- 52 C. J. Brabec, A. Cravino, D. Meissner, N. S. Sariciftci, T. Fromherz, M. T. Rispens, L. Sanchez and J. C. Hummelen, *Adv. Funct. Mater.*, 2001, **11**, 374–380.
- 53 K. Walzer, B. Maennig, M. Pfeiffer and K. Leo, *Chem. Rev.*, 2007, **107**, 1233–1271.
- 54 V. Shrotriya, Y. Yao, G. Li and Y. Yang, *Appl. Phys. Lett.*, 2006, **89**, 063505.
- 55 M. Weidelener, C. D. Wessendorf, J. Hanisch, E. Ahlswede, G. Götz, M. Lindén, G. Schulz, E. Mena-Osteritz, A. Mishra and P. Bäuerle, *Chem. Commun.*, 2013, **49**, 10865–10867.

- 56 J. Cao, Q. Liao, X. Du, J. Chen, Z. Xiao, Q. Zuo and L. Ding, *Energy Environ. Sci.*, 2013, **6**, 3224.
- 57 I. Horcas, R. Fernández, J. M. Gómez-Rodríguez, J. Colchero, J. Gómez-Herrero and A. M. Baro, *Rev. Sci. Instrum.*, 2007, **78**, 013705.
- 58 CryaAlis<sup>Pro</sup>, Agilent Technologies XRD Products.
- 59 O. V. Dolomanov, L. J. Bourhis, R. J. Gildea, J. A. K. Howard and H. Puschmann, *J. Appl. Cryst.*, 2009, **42**, 339-341

## Table of contents



A new class of A-D-A molecular donor materials based on planar *S,N*-heterohexacene is developed for vacuum-processed planar and bulk-heterojunction solar cells providing promising power conversion efficiencies up to 7.1%.